

Multi-modal Residual Perceptron Network for Audio-Video Emotion Recognition

Xin Chang, Władysław Skarbek

Warsaw University of Technology, Institute of Radioelectronics and Multimedia Technology
 * xin.chang.dokt@pw.edu.pl

Abstract: Emotion recognition is an important research field for Human-Computer Interaction(HCI). Audio-Video Emotion Recognition (AVER) is now attacked with Deep Neural Network (DNN) modeling tools. In published papers, as a rule, the authors show only cases of the superiority of multi modalities over audio-only or video-only modalities. However, there are cases superiority in single modality can be found. In our research, we hypothesize that for fuzzy categories of emotional events, the higher noise of one modality can amplify the lower noise of the second modality represented indirectly in the parameters of the modeling neural network. To avoid such cross-modal information interference we define a multi-modal Residual Perceptron Network (MRPN) which learns from multi-modal network branches creating deep feature representation with reduced noise. For the proposed MRPN model and the novel time augmentation for streamed digital movies, the state-of-art average recognition rate was improved to 91.4% for The Ryerson Audio-Visual Database of Emotional Speech and Song(RAVDESS) dataset and to 83.15% for Crowd-sourced Emotional multi-modal Actors Dataset(Crema-d). Moreover, the MRPN concept shows its potential for multi-modal classifiers dealing with signal sources not only of optical and acoustical type.

Keywords: emotion recognition; deep neural network; multi-modal classifier; deep features fusion; audio sensor; video sensor



Citation: Chang, X.; Skarbek, W. Multi-modal Residual Perceptron Network for Audio-Video Emotion classification. *Preprints* 2021, 1, 0. <https://doi.org/>

Received:
 Accepted:
 Published:

Publisher's Note: MDPI stays neutral with regard to jurisdictional claims in published maps and institutional affiliations.

arXiv:2107.10742v1 [eess.SP] 21 Jul 2021

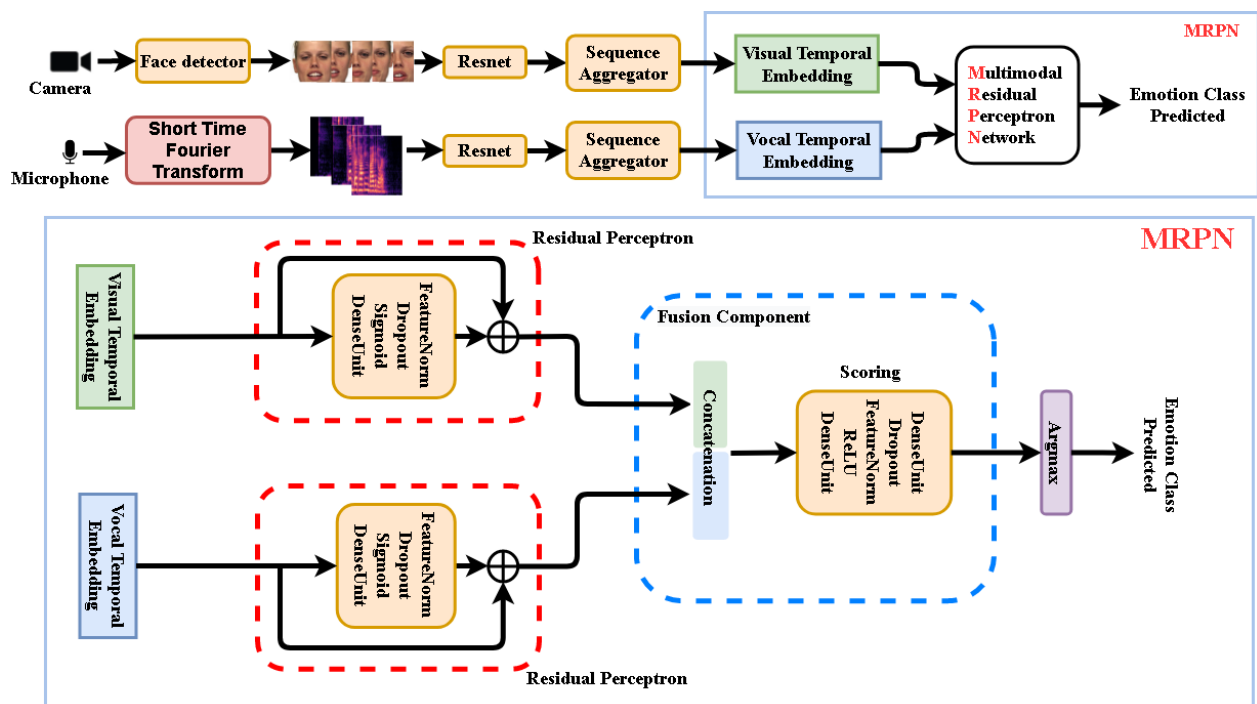


Figure 1. The proposed multi-modal emotion recognition system using Deep Neural Network (DNN) approach. **Upper part:** Video frames and audio spectral segments get independent temporal embeddings to be fused by our multi-modal Residual Perceptron Network (MRPN). **Lower part:** MRPN performs in each modality normalizations via the proposed Residual Perceptrons and then scores their concatenated outputs in the Fusion Component.

1. Introduction

This paper presents a novel end-to-end DNN based framework, as Figure 1 illustrates, addressing the AVER problem. Just like human beings understand emotional expressions in our daily social activities through multi-senses (e.g., visual, vocal, textually meaningful), neural computing units as part of intelligent artificial sensors are now playing important roles in emotion recognition tasks. Specialized sensors in HCI capture information responsible for understanding visual and vocal information just like we – the human beings – understand emotional expressions through our multi-senses.

1.1. Emotion recognition from face expression and voice timbre

Intuitively, functionalities of intelligent artificial neurons are assigned with similar concepts as our brain cells, processing information from the very raw senses independently and appropriately to their types.

Visually, information captured by the camera is distributed to several frames as Figure 2 shows. Discrete information in a single frame is firstly delivered to pattern extracting intelligent sensors for features such as Fisherfaces and Eigenfaces[1] or the deep features from Convolution Neural Network(CNN)[2]. To fully preserve the information from the discrete signals, some Sequence Aggregation Component(SAC), e.g., Long Short Term Memory(LSTM)[3] or Transformer[4], is then needed to further process the extracted features. Finally, a classifier such as Support Vector Machine(SVM) or some neural dense layer takes the integrated features for the classification.



Figure 2. Video frames of visual facial expressions selected from RAVDESS dataset.

Raw vocal inputs are usually with 10,000 to 44,100 samples per second, while the visual frame rate is about 25-30 image frames per second. Though raw digital signals in the time domain approximate the original signal precisely, their spectral representation, e.g., Spectrogram frame, Mel-spectrogram coefficients, or Log Mel-spectrogram frame, appeared more effectively for sound recognition. The spectral converted vocal signals have shown significant improvements in many classification problems, in spite of some limitations. Due to the fact that expression events do not last at the same time, the width of the Spectrogram frames is changing, what is not desirable for CNN pattern extractors. Therefore we also need some help from a SAC which outputs integrated features. Figure 3 shows the expression events from different categories and time duration.

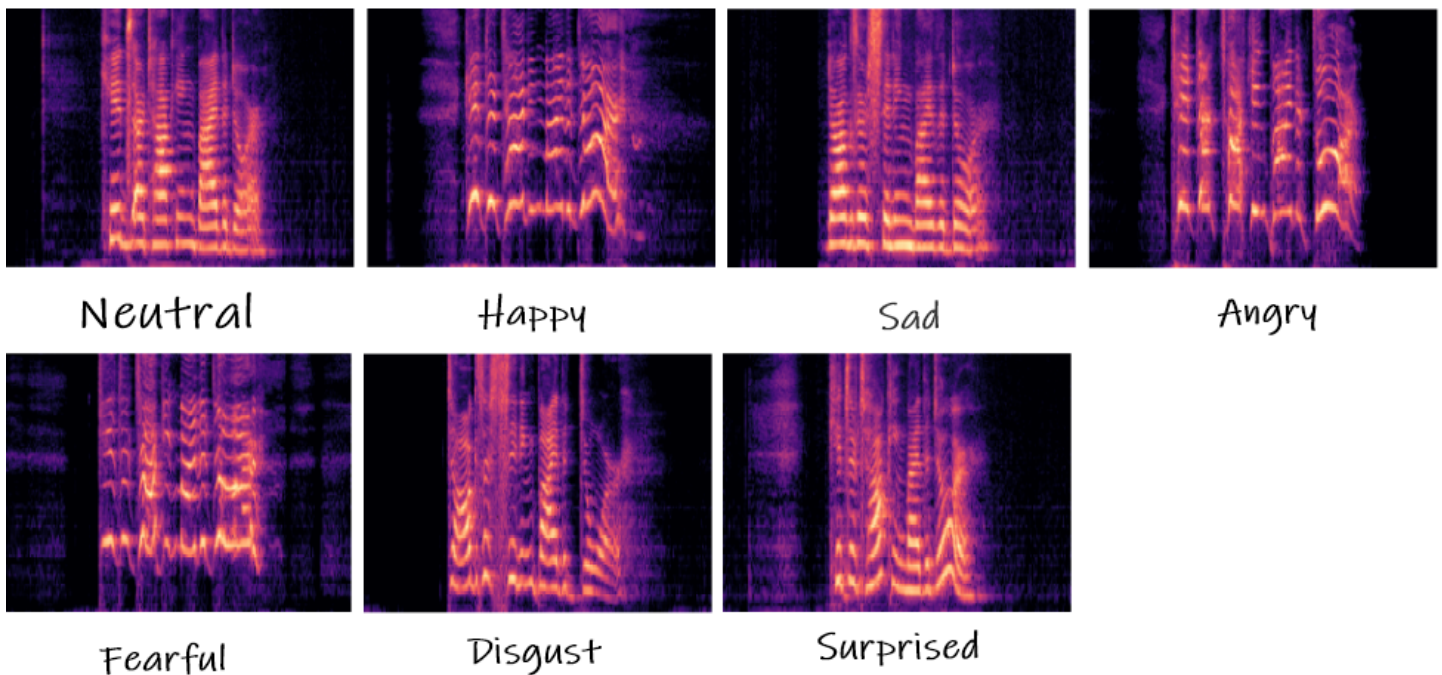


Figure 3. Mel Spectrograms of vocal timbres selected from RAVDESS dataset.

1.2. Multi-modal emotion recognition

AVER solution also follows the sensation of human beings, people claim they hear the sound when looking at the sheet music, smell the odor when recalling the memory from a photo or see the sea sight from the smell of the air. The multi-sensation information is processed by different areas of our cerebral cortex, movement, hearing, seeing, and so on, then highly correlated by some other brain areas. The learning process of neural sensors also mimics our learning process. The neurons shape their weights just like our cerebral cortex changes from the stimulation of the environments during the learning process in the supervised neural network sensors training. Many have shown significant improvement of multi-modal solutions.

N. Neverova et al.[5] suggest gradual fusion involving the random dropping of separate channels, and this method was adopted by V. Vielzeuf et al. [6] in the AVER solution for their best result. Fusion at early or late-stage is discussed by R. Beard et al.[7]. A. Zadeh et al [8] proposed Multi-view Gated Memory to gate the multi-modal knowledge from LSTM in the time series.

S. Zhang et al.[9] take features from CNN and 3D-CNN models for vocal and visual sources then make global averaging as video features. E. Tzinis et al.[10] take cross-modal and self-attention modules, Y. Wu et al.[11] localize events crossing modalities.

[11–14] have all adopted concatenation as a simple fusion of deep features from visual and vocal modalities in the AVER solution. This, however, leads to a potential deficiency of cross-modal information interference.

1.3. Cross-modal information interference

Let's consider the human brain learning process again. Say the information is wrong in any of the sensory stimulation. A child learned an animal looks just like a dog but having the sound of the cat from the manipulated movies and this kid has never learned the dog and cat in a real-life environment. He will either see a dog and tell it's a cat or hear the cat sound and tell it's a dog. His cognition is surely wrong in such a scenario.

His recognition is still intact to some extent that he can recognize the visual or acoustic information pattern. But the recognized information is corrupted, along with the correlation of the cross-modal information. This made the corrupted single modal knowledge he learned having also a negative impact on the other. The same concept we address to the current multi-modal neural network architecture. If any of the simulations is fuzzy, not just it will corrupt the single modality neuron weights, but also the feature fusion neurons that correlate cross-modal knowledge and eventually damage other modalities. F. Ma[15] has shown that controlled missing information in some modalities can decrease the recognition performance, while we argue there is much uncontrolled misleading information in the multi-modal neuron approach.

1.4. Paper contribution and structure

With the consideration mentioned, we demonstrate how this kind of misleading information is fed to the neural network system and propose a novel mechanism to prevent it. According to the framework, data processing and optimized network training strategy are discussed. And finally, the detailed analysis and discussion are presented by computing experiments on the RAVDESS and Crema-d datasets. Our major contributions are concluded as follows:

1. *Multi-modal framework*: We propose a novel within-modality Residual Perceptrons (RP) that exploits multi-branch gradients flows for the multi-modal neural network optimization. The combination of sub-networks and loss functions produces superior parameterized multi-modal features. Not just the framework eliminating the cross-modal information interference, but also easier to be optimized during training compared with training each modality separately.
2. *Time Augmentation of input frames*: We demonstrate data augmentation in time involving randomly slicing over input frame sequences from both modalities, which improved the recognition performance to the state-of-art, even without MRPN. Additionally, due to the elimination of the cross-modal information interference by MRPN, visual and vocal inputs can pair from different movie sources to make the learned multimodal features more general. These data augmentation strategies made our network enough robust to a reduced number of training movies.

2. Hypothesis on Cross-modal Information Interference

In this section, we discuss our hypothesis where mismatching information from the modalities can cause chaos in the correlation neurons, namely the fusion component, and eventually broadcast such erroneous signals to the single modal neurons in the multi-modal solutions in AVER.

2.1. Fuzziness of the information adopted in single modal emotion recognition approach

The insufficient or fuzzy information can be noticed in either visual or vocal modality emotion recognition solution, and then the success rate of recognition can not be increased noticeably.

Namely, the visual modality results from the challenge FER-2013 [16] for single image facial recognition have only improved about 4% to 76.8% over the past eight years by W. Wang et al. [17].

Moreover, for video frames, HW. Ng et al. [18] got 47.3% validation accuracy and 53.8% testing accuracy on EmotiW dataset [19] using transfer learning and averaged temporal deep features.

Similarly for vocal solutions, the results for Interactive Emotional Dyadic Motion Capture dataset (IEMOCAP) [20] with the raw inputs are reported around 76% by S. Kwon [21] and 64.93% by S. Latif et al. [22]. The recognition rate for these cases is far from optimal.

Apart from the design, functionality, and training of the neural network, the human voting for those datasets draws our concerns. As the teacher in supervised learning, almost all datasets related to emotion recognition have unsatisfactory knowledge. The ones who understand human emotions the best, the human beings themselves, cannot make a majority of the agreement to the author's labeling. On average, the human rate of the emotional categories is 72% from IEMOCAP, human accuracy on FER-2013 [16] was $65 \pm 5\%$, Crema-d [23] holds the accuracy of 63.6% and RAVDESS [24] has the results of 72.3%.

All the reports pointed out that in every single modality, the information of data is never crystal, thus the learned knowledge of a single modality in emotion recognition, can be corrupted and uncontrolled by the network. We can't identify or agree on which samples are wrong because the boundaries of the clusters are quite subjective. Figure 4 illustrates some confusing emotional samples from visual modality.

Multi-modal solutions seem to clarify the fuzziness of the information where we correlate the sensations from multi-sources. All have reported the improvements of multi-modal solutions. However, we hypothesize that the fused features have amplified noise comparing to single modality features due to the correlating processing, the side effects are concealed by its benefits.

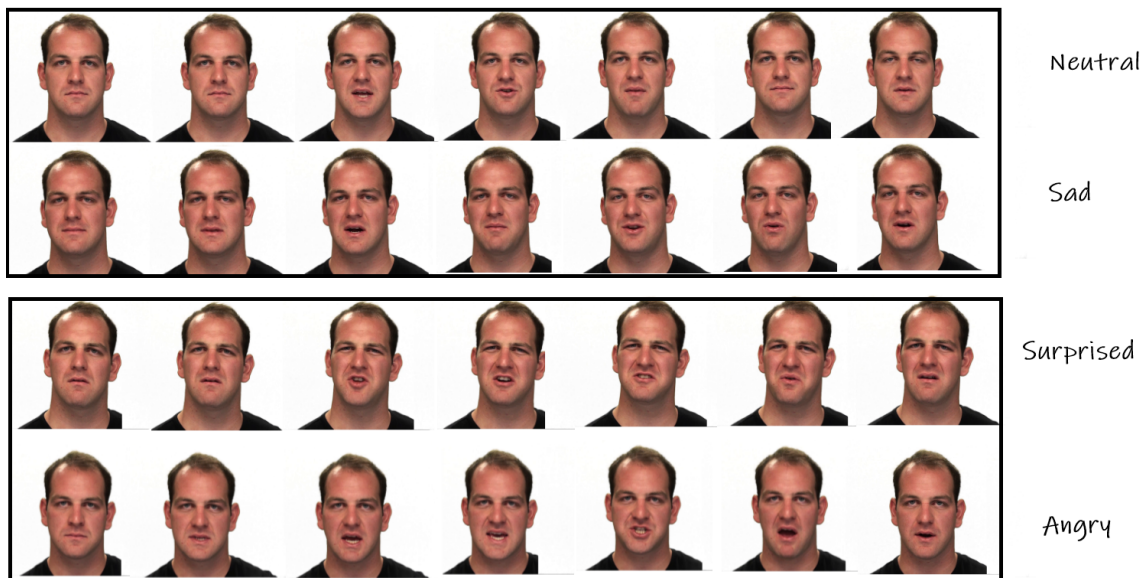


Figure 4. Selected RAVDESS visual frames with assigned controversial labels of emotion classes.

Figure 5 shows us the significant clustering improvements from the multi-modal solution of simple multi-modal features concatenation over the single modality solutions.

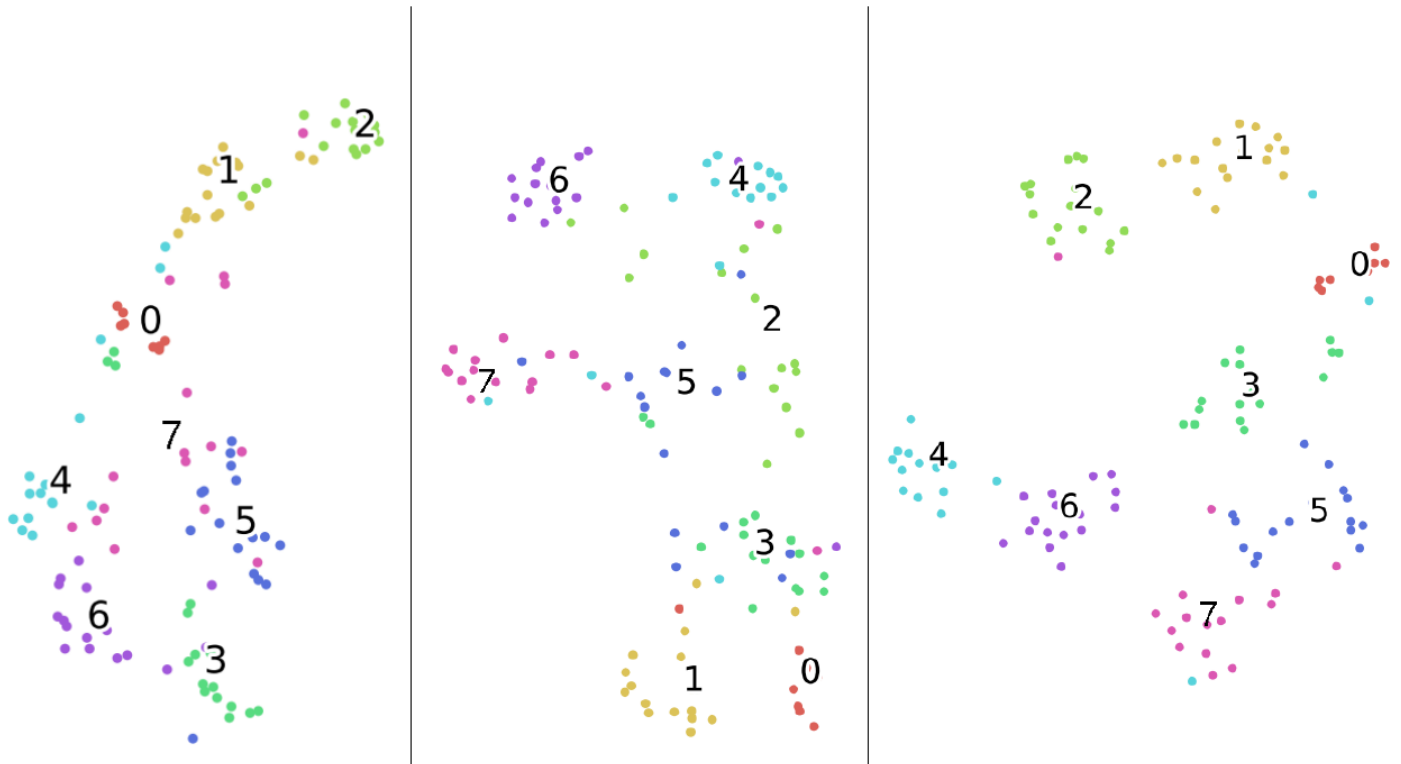


Figure 5. Visualization (t-SNE algorithm) of deep features clustering with respect to emotion classes, where 0: *neutral*, 1: *calm*, 2: *happy*, 3: *sad*, 4: *angry*, 5: *fearful*, 6: *disgust*, 7: *surprised*. **Left part:** only image modality. **Middle part:** only audio modality. **Right part:** image and audio modalities fused.

2.2. Information disagreement in single modalities

From Figure 5 We can also observe that based on the same training and testing data, the visual modality and vocal modality is having different clustering, where sad (3) expression clusters are closed to disgust (6) and fearful (5) clusters in the visual modality while they are closed to calm (1) and neutral (0) expression clusters in vocal modality, some misclassification cases also happen between the nearest neighbors. The clustering results show that some information in the visual inputs and vocal inputs do not align with the labels we used to teach neural networks. Thus the learned data examples have the same deficiency we have shown by the dog and cat example in the subsection on *Cross-modal information interference* 1.3.

These clustering results prove again the fuzziness of information in every single modality. The learned fuzzy knowledge of the classifier caused wrong clustering of the nearest neighbors as we see in Figure 5, indicating the mismatching of information for either training or testing samples to their labels.

Especially in DNN solutions, since we propagate and nest all the trainable parameters, effectively fuse features from different modalities, we have no control in broadcasting knowledge from one modality to the others. Then we get a high probability chance to amplify the noisiness of the data.

2.3. Deficiency of simple multimodal features concatenation

Figure 6 illustrates the problem of cross-modal information interference during gradient backpropagation, wherein the blue frame denotes the fusion component. Namely, the concatenation unit of the features from different modalities can backpropagate the gradients modifying jointly weights in each modality. In such a case the knowledge of each modality before the fusion layer can differ from the knowledge learned in the case of a single-modality solution.

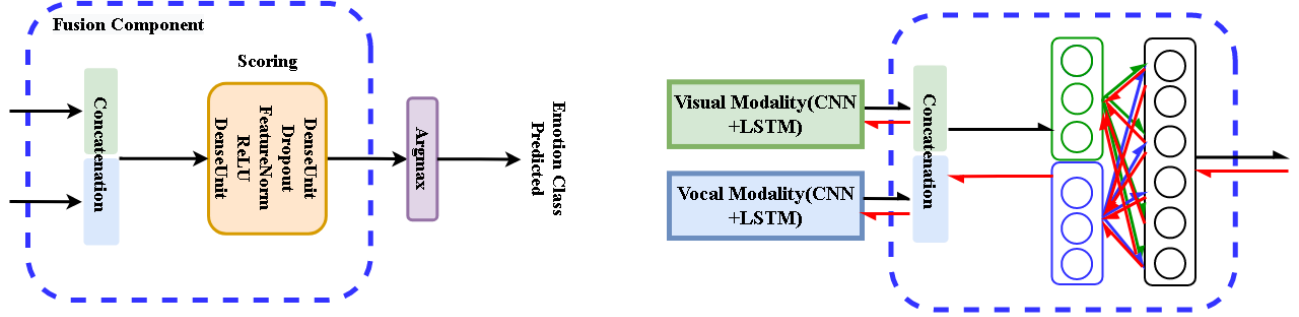


Figure 6. Cross-modal information interference of gradients backpropagation due to the fusion layers. The gradients from fused layer makes impact on gradients flow into neural weights of both modalities.

In general, in the case of the knowledge in some modalities, but not all modalities, is fuzzy, the noise can be introduced cross modalities to the clean modalities for such samples.

3. Proposed Methods

Addressing the mentioned issues, we proposed a novel MRPN along with multi-branch loss functions to demonstrate the improvements in preventing cross-modal interference.

3.1. Functional description of analyzed networks

The functional descriptions of the analyzed deep networks are presented for their training mode (see Figure 7). They are based on the selected functionalities of neural units and components. We use index m for inputs of any modality. In our experiments $m = v$ or $m = a$.

1. F_m : feature extractor for input temporal sequence x_m of modality m , e.g. F_v for video frames x_v , F_a for audio segments x_a .
2. A_m : aggregation component SAC for temporal feature sequence leading to temporal feature vector f_m , eg. A_v , A_a for video and audio features, respectively.

$$f_m \doteq A_m(F_m(x_m)) \longrightarrow f_v \doteq A_v(F_v(x_v)), f_a \doteq A_a(F_a(x_a)) \quad (1)$$

3. Standard computing units: DenseUnit – affine (a.k.a. dense, full connection), Dropout – random elements dropping for model regularizing, FeatureNorm – normalization for learned data regularizing (batch norm is adopted in the current implementation), and Concatenate – joining feature maps, ReLU, Sigmoid – activation units.
4. Scoring – component mapping feature vectors to class scores vector, usually composing the following operations:

$$\rightarrow \text{DenseUnit} \rightarrow \text{ReLU} \rightarrow \text{FeatureNorm} \rightarrow \text{DenseUnit} \quad (2)$$

$$\begin{aligned} m \in \{v, a\}, \hat{f}_m &\doteq \text{FeatureNorm}(f_m) \longrightarrow s_m \doteq \text{Scoring}(\hat{f}_m) \\ g_{va} &\doteq \text{FeatureNorm}(\text{Concatenate}(g_v, g_a)) \longrightarrow s_{va} \doteq \text{Scoring}(g_{va}) \end{aligned} \quad (3)$$

5. **FusionComponent** – concatenates its inputs g_v, g_a , then makes the statistical normalization, and finally produces the vector of class scores:

$$\begin{aligned} s_{va} &\doteq \text{FusionComponent}(g_v, g_a) \longrightarrow \\ g_v, g_a &\rightarrow \text{Concatenate} \rightarrow \text{Scoring} \rightarrow s_{va} \end{aligned} \quad (4)$$

In our networks g_v, g_a are statistically normalized multi-modal features or their residually updated form.

6. **SoftMax** – computing unit for normalization of class scores to class probabilities:

$$\begin{aligned} m \in \{v, a\} &\longrightarrow p_m \doteq \text{Softmax}(s_m) \\ p_{va} &\doteq \text{Softmax}(s_{va}) \end{aligned}$$

7. **CrossEntropy** – a divergence of probability distributions used as loss function. Let p is the target probability distribution. Then the following loss functions are defined:

$$\begin{aligned} m \in \{v, a\}, p_m &\doteq \text{Softmax}(s_m) \longrightarrow \mathcal{L}_m \doteq \text{CrossEntropy}(p, p_m) \\ p_{va} &\doteq \text{Softmax}(s_{va}) \longrightarrow \mathcal{L}_{va} = \text{CrossEntropy}(p, p_{va}) \\ \mathcal{L} &\doteq \mathcal{L}_v + \mathcal{L}_a + \mathcal{L}_{va} \end{aligned} \quad (5)$$

8. **ResPerceptron (Residual Perceptron)** – component performing statistical normalization for the dense unit (perceptron) computing residuals for normalized data. In our solution it transforms a modal feature vector f_m into f'_m , as follows:

$$\begin{aligned} \hat{f}_m &\doteq \text{FeatureNorm}(f_m) \longrightarrow f'_m \doteq \text{ResPerceptron}(\hat{f}_m) \longrightarrow \\ f'_m &\doteq \hat{f}_m + \text{FeatureNorm}(\text{Sigmoid}(\text{DenseUnit}(\hat{f}_m))) \end{aligned} \quad (6)$$

Three networks $\mathcal{N}_0, \mathcal{N}_1, \mathcal{N}_2$ are defined for further analysis:

1. Network $\mathcal{N}_0(f_v, f_a; p)$ with fusion component and loss function \mathcal{L}_{va} :

$$\begin{aligned} \hat{f}_v &\doteq \text{FeatureNorm}(f_v), \hat{f}_a \doteq \text{FeatureNorm}(f_a) \\ s_{va} &\doteq \text{FusionComponent}(\hat{f}_v, \hat{f}_a) \\ p_{va} &\doteq \text{SoftMax}(s_{va}) \longrightarrow \mathcal{L}_{va} \doteq \text{CrossEntropy}(p, p_{va}) \end{aligned} \quad (7)$$

2. Network $\mathcal{N}_1(f_v, f_a; p)$ with fusion component and fused loss function $\mathcal{L} \doteq \mathcal{L}_v + \mathcal{L}_a + \mathcal{L}_{va}$:

$$\begin{aligned} \hat{f}_v &\doteq \text{FeatureNorm}(f_v), \hat{f}_a \doteq \text{FeatureNorm}(f_a) \\ s_v &\doteq \text{DenseUnit}(\hat{f}_v), s_a \doteq \text{DenseUnit}(\hat{f}_a), s_{va} \doteq \text{FusionComponent}(\hat{f}_v, \hat{f}_a) \\ p_v &\doteq \text{SoftMax}(s_v) \longrightarrow \mathcal{L}_v \doteq \text{CrossEntropy}(p, p_v) \\ p_a &\doteq \text{SoftMax}(s_a) \longrightarrow \mathcal{L}_a \doteq \text{CrossEntropy}(p, p_a) \\ p_{va} &\doteq \text{SoftMax}(s_{va}) \longrightarrow \mathcal{L}_{va} \doteq \text{CrossEntropy}(p, p_{va}) \end{aligned} \quad (8)$$

3. Network $\mathcal{N}_2(f_v, f_a; p)$ with normalized residual perceptron, fusion component and fused loss function $\mathcal{L} \doteq \mathcal{L}_v + \mathcal{L}_a + \mathcal{L}_{va}$:

$$\begin{aligned}
\hat{f}_v &\doteq \text{FeatureNorm}(f_v), \hat{f}_a \doteq \text{FeatureNorm}(f_a) \\
f'_v &\doteq \text{ResPerceptron}(\hat{f}_v), f'_a \doteq \text{ResPerceptron}(\hat{f}_a) \\
s_v &\doteq \text{DenseUnit}(\hat{f}_v), s_a \doteq \text{DenseUnit}(\hat{f}_a), s_{va} \doteq \text{FusionComponent}(f'_v, f'_a) \\
p_v &\doteq \text{SoftMax}(s_v) \longrightarrow \mathcal{L}_v \doteq \text{CrossEntropy}(p, p_v) \\
p_a &\doteq \text{SoftMax}(s_a) \longrightarrow \mathcal{L}_a \doteq \text{CrossEntropy}(p, p_a) \\
p_{va} &\doteq \text{SoftMax}(s_{va}) \longrightarrow \mathcal{L}_{va} \doteq \text{CrossEntropy}(p, p_{va})
\end{aligned} \tag{9}$$

For the networks $\mathcal{N}_0, \mathcal{N}_1, \mathcal{N}_2$ detailed in Figure 7, we can observe:

1. All instances of *FeatureNorm* unit are implemented as batch normalization units.
2. In testing mode only the central branches of networks $\mathcal{N}_1, \mathcal{N}_2$ are active while the side branches are inactive as they are used only to compute the extra terms of the extended loss function.
3. The above facts make network architectures $\mathcal{N}_0, \mathcal{N}_1$ equivalent in the testing mode. However, the models trained for those architectures are not the same, as weights are optimized for different loss functions.
4. In the testing mode all *Dropout* units are not active, as well.
5. The architecture of *FusionComponent* is identical for all three networks. The difference between models of \mathcal{N}_0 and \mathcal{N}_1 networks follows from the different loss functions while the difference between models of \mathcal{N}_1 and \mathcal{N}_2 networks is implied by using *ResPerceptron (RP)* components in \mathcal{N}_2 network.
6. To control the range of affine combinations computed by *Residual Perceptron (RP)* component, we use *Sigmoid* activations instead of the *ReLU* activations exploited in other components. The experiments confirm the advantage of this design decision.
7. The *Residual Perceptron (RP)* was introduced in the network \mathcal{N}_2 to implement parametrized normalization of modal features before their fusion. RP was designed when other attempts of multi-modal features normalization for fusion was not successful. For instance, the Siamese Network [25] was tested. We expected that minimizing distances between features from different modalities could lead to the higher matching of class scores for audio and video data. However, this intuition appeared to be invalid.

3.2. MRPN in general multi-modal tasks

We suggest that MRPN can be adopted in any multi-modal task that involves many multi-modal input sources and one target function or many multi-modal inputs and many multi-modal target functions as Figure 8 shows. In both cases MRPN is served as an advanced correlator, by having as many sub-loss functions as constraints, MRPN can form integrated features better than a simple concatenation mechanism if single modality features are highly correlated. Otherwise, sub-loss functions can still reduce the cross-modal information interference from any of the input sources.

3.3. Pre-processing

Our data pre-processing includes the procedure for both modality inputs, namely spatial and time-dependent augmentation are applied.

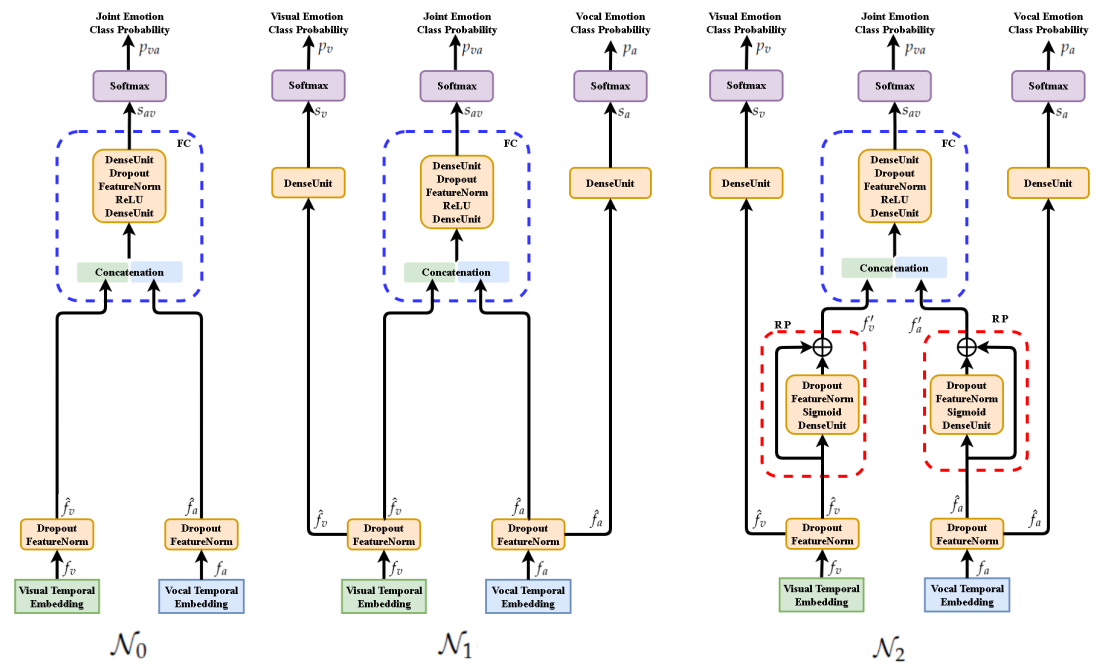


Figure 7. Evolution of network design for multi-modal fusion (presented for training mode). \mathcal{N}_0 : Fusion component (FC) only. \mathcal{N}_1 : Beside FC, independent scoring of each modality is considered. \mathcal{N}_2 : Extending \mathcal{N}_1 network by Residual Perceptrons (RP) in each modality branch.

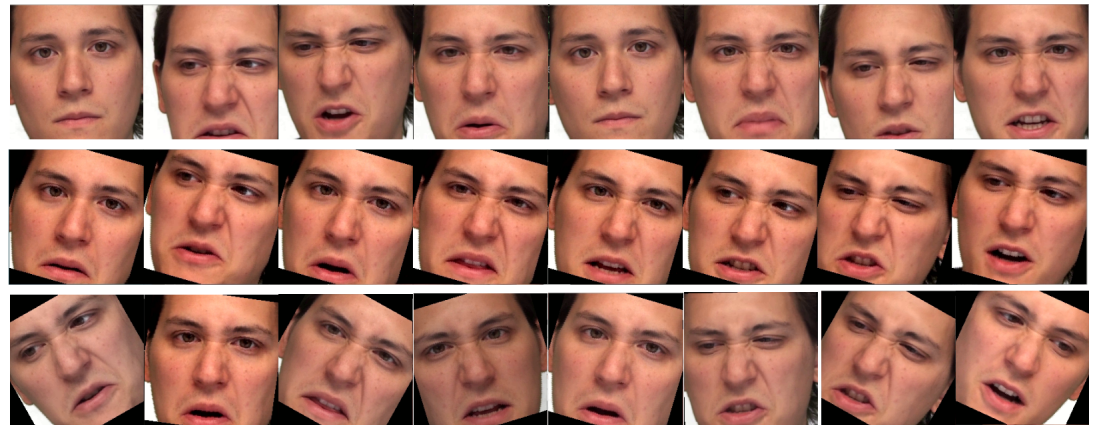


Figure 9. Visual comparison of augmentation procedure for cropped video frames. **Top part:** original video frames. **Middle part:** applying random augmentation parameters – same for all frames. **Bottom part:** applying random augmentation parameters – different for each frame.

1. *Spatial data augmentation for visual frames:*
The facial area for the visual input frames is cropped using a CNN solution from Dlib library [26]. Once the facial area is cropped, spatial video augmentation is applied during the training phase. The same random augmentation parameters are applied for all frames of a video source illustrated in Figure 9.
2. *Time dependent data augmentation for visual frames:*
Obviously, expressions from the same category do not last the same duration. To make our system robust to the inconsistent duration of the emotion events, we perform data

augmentation in time by randomly slicing the original frames as Figure 10 illustrates. Such operation should also avoid too few input frames missing information of the expression events. Thus the training segments are selected to have at least one-second duration unless the original duration of the file is less than that.

3. *Spatial data augmentation for vocal frames:*

Raw audio inputs are resampled at 16kHz and standardized by their mean and standard deviation without any denoising or cutting to remove influence from the distance of the speaker to the microphone, or subjective base volume of the speaker. The standardized wave is then divided into one-second segments and converted to spectrograms by a Hann windowing function of size 512 and hop size of 64.

The above facts specify the size of the spectrogram at 256×250 , approaching the required input shape of Resnet-18 – the CNN extractor used in our experiment. The chunk size using such inputs for Resnet-18 [27] is close to its desired performance utilizing the advantage in the middle deep features.

4. *Time dependent augmentation for vocal frames:*

Similar to the time augmentation in visual inputs, raw audio inputs are also randomly sliced. The raw data is further over-sampled in both the training and testing mode by a hopping window. A window of 0.2 seconds, 1/5 duration of the input segments to the CNN extractor is specified. The oversampling further improved our results by the increasing number of deep features from the output deep feature sequences of CNN to the SAC. The mechanism grants the opportunity for the sequence aggregator SAC to investigate more details of the temporal information in the deep feature vectors.

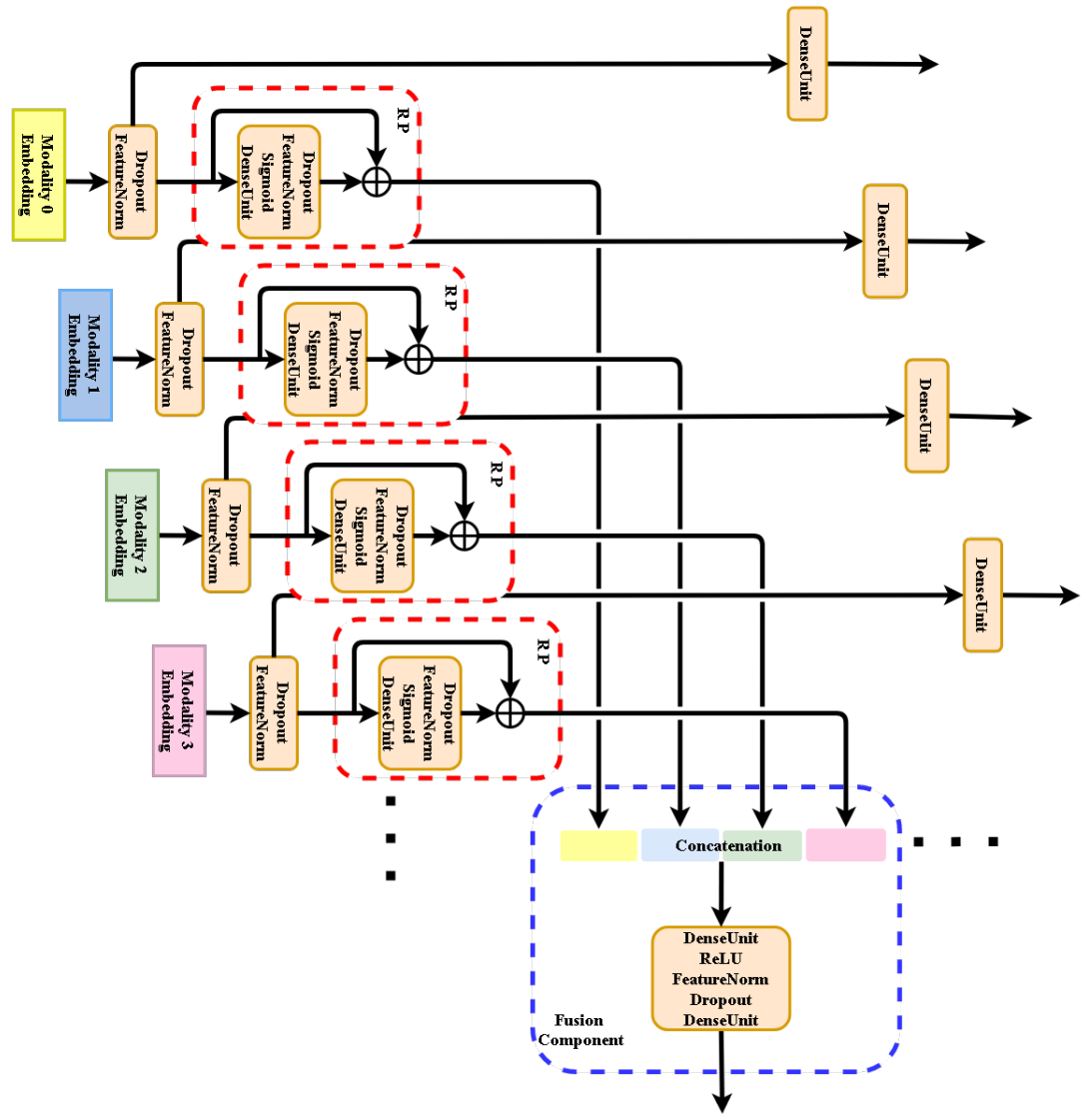


Figure 8. Generalization of our MRPN fusion approach to many modalities. It could be used for either regression or classification tasks.



Figure 10. Examples of time dependent augmentation for visual frames. **Top part:** original frames. *Middle part:* sliced frames start at beginning of the original frames. **Bottom part:** sliced frames start at the middle of the original frames.

4. Computational Experiments and their Discussion

This section presents an evaluation regarding the advantages of our proposed framework and time-dependent augmentation. Two datasets, RAVDESS and Crema-d are employed for this purpose. The improvement of the time-augmentation mechanism is analyzed in the baseline model which brought us state-of-art results even without MRPN design. The inferior cases in such common neural multi-modal solutions are detected and discussed in the comparison. Improvement of preventing the cross-modal information interference cases by MRPN is then presented, not just in the detected inferior sub-datasets, but also in general data samples.

4.1. Datasets

RAVDESS and Crema-d differ in numbers of expression categories, total files, identifies, and also video quality.

1. RAVDESS dataset includes both speech and song files. For the speech recognition proposal, we only use the speech files from the dataset. It contains 2880 files, 24 actors (12 female, 12 male), state two lexically identical statements. Speech includes calm, happy, sad, angry, fearful, surprise, and disgusted expressions. Each expression is produced at two levels of emotional intensity (normal, strong), with an additional neutral expression, in a total of 8 categories. It is the most recent video-audio emotional dataset with the highest video quality in this research area to our best knowledge.
2. Crema-d dataset consists of visual and vocal emotional speech files in a range of basic emotional states (happy, sad, anger, fear, disgust, and neutral). 7,442 clips of 91 actors with diverse ethnic backgrounds were rated by multiple raters in three modalities: audio, visual, and audio-visual.

For both datasets, the training set and testing set are separated using the similar concepts as 10-fold cross-validation. Additionally, identities of the actors are also separated in train and val sets to prevent the results leaning on the actors. Around 10% of the actors are used for validation while the remaining 90% are used for training, male and female actors are balanced in each set. We rotate the split train/validation sub-datasets to get multiple results over the whole datasets.

Crema-d dataset has fewer categories for the classification tasks, but from the report of the authors themselves, Crema-d holds the accuracy of 63.6% from human recognition for 6 categories which less than RAVDESS at 72.3% for 8 categories. The resolution of the video source is verified not the cause of the worse performance. The better results in the RAVDESS

dataset, from our opinion, is the more crystal and natural emotion information inside the RAVDESS dataset.

4.2. Model organization and computational setup

The baseline model \mathcal{N}_0 , advanced fusion network \mathcal{N}_1 and the \mathcal{N}_3 (MRPN) have the same CNN extractors at the initial stage of the training. To compare the impact of strategy from features fusion only, CNN extractor architecture is fixed to Resnet-18 [27].

The CNN in visual modality is initialized from a facial image expression recognition task, the challenge FER2013 [16]. As for vocal modality, The CNN is pretrained on the voice recognition task from VoxCeleb dataset [28]. The initialization of the CNN extractors made the whole system much easier to be optimized.

AdaMW optimizer is adopted for the model optimization, with the initial learning rate at $5 \cdot 10^{-5}$, decreased two times if validation loss is not dropping over ten epochs.

4.3. Improvement of time-dependent data augmentation

This subsection illustrates the improvement of time-dependent augmentation. The single modality solutions in our experiment (shown in Table 1) take pretrained Resnet-18 as extractors and LSTM cells as SACs. The simple multi-modal solution takes twice of the components with an additional fusion layer as Figure 7 illustrates on the left panel. Adopting time-dependent augmentation shows overall performance improvements on either single or multi-modal solutions.

The Table notations are presented in the follows:

In the variational train/val sub-datasets in Table 1, Ax,y stands for the validation files that came from actor x and y, odd number notes for a male actor, and even number for a female actor.

Table 1. Comparison of single modalities models with \mathcal{N}_0 model (RAVDESS cases): VM – Visual Modality only, AM – Audio Modality only, JM – Joint Modalities (\mathcal{N}_0 model), T – having time augmentation by signal random slicing, NT – not having time augmentation.

RAVDESS	A1,2	A3,4	A5,6	A7,8	A9,10	A11,12
AM(NT)	70.8%	55.0%	57.5%	74.1%	43.5%	65.8%
AM(T)	71.6%	77.5%	71.6%	90.0%	55.8%	69.1%
VM(NT)	82.5%	70.0%	66.7%	74.1%	80.3%	63.3%
VM(T)	86.6%	75.0%	70.6%	76.6%	87.3%	69.1%
JM(NT)	90.8%	89.1%	85.2%	89.3%	78.5%	85.5%
JM(T)	97.5%	90.3%	87.5%	97.5%	86.5%	87.5%
RAVDESS	A13,14	A15,16	A17,18	A19,20	A21,22	A23,24
AM(NT)	59.8%	57.5%	57.5%	55.5%	68.3%	63.3%
AM(T)	70.0%	69.1%	51.6%	63.3%	55.8%	68.3%
VM(NT)	71.3%	60.0%	63.3%	70.8%	65.8%	70.8%
VM(T)	73.3%	65.0%	64.1%	78.3%	66.6%	74.1%
JM(NT)	77.5%	75.5%	76.3%	85.2%	82.8%	80.0%
JM(T)	82.4%	79.6%	83.2%	89.0%	85.5%	84.2%

We would like to throw a discussion on whether visual and vocal information should align in time. We believe the recognition of the expression shouldn't depend on the duration of the expression events, thus slicing and shifting the inputs in the time axis is natural. Some people might suggest the information align, just like Mansouri-Benssassi and Ye [29] proposed

early solution for avoiding cross-modal information interference. E. Ghaleb [30] makes fusion in each segment from the sequences. Though the alignment ensures the naturality of the data, it's also natural if the subjects we study have stopped speech yet showing some facial expression, or otherwise. Thus making the nonalignment of the sequences in the two modalities in fact make better generalization of their correlation. Though individual modality branches should expect the same learned knowledge, the feature fusion correlator can expect more general knowledge from the mentioned mechanism.

4.4. Discussion on inferior multi-modal cases

Our hypothesis came from the time augmentation evaluation in Table 1. In the case of A9,10, visual modality is having better results than a multi-modal solution in either solution whether or not having time-dependent augmentation. Notice the degeneration of the performance does not depend on the data, but only on the modalities. The inferior case indicating the extra vocal modality information we brought, somehow decreased the recognition rate of the system.

We argue such deficiency is common in fuzzy multi-modal data, as we discussed in subsection *Information disagreement in single modalities* 2.2 and showed in Figure 5. The pattern learning ability from both modalities is well enough, both solutions have performance over 85% in cases like A7,8 and A1,2. But when the data information became fuzzy, the learned knowledge in the single modality solution is poisoned and is broadcasted to the other modalities as we discussed in subsection *Deficiency of simple multimodal features concatenation* 2.3 shown by Figure 6.

The inferior case is only shown once in the sub-datasets but it doesn't mean there are only a few noisy samples. The degeneration became visible from the model performance only because the percentage of the noisy samples has passed some kind of threshold in the training set. If so, by eliminating or reducing such side effects, overall improvements should be expected for any train and testing sub-dataset.

4.5. Performance of multi-modal Residual Perceptron Network

This subsection addresses the improvement of MRPN preventing the multi-modal information interference we hypothesized. MRPN serves as an advanced correlator for the multi-modal deep features, similar to Tang et al.[31] performs adversarial neural attack at the deep feature level. The operation assumes the MRPN components only perform correlation function, where all mapping functionalities for the single modalities are performed before it, constrained by our multi-branch loss functions in the other branches discussed in subsection *Functional description of analyzed networks* 3.1.

Table 2. Comparison for RAVDESS of MRPN approach (network \mathcal{N}_2) with simple fusion strategy (\mathcal{N}_0), and advanced fusion strategy (\mathcal{N}_1).

RAVDESS	A1,2	A3,4	A5,6	A7,8	A9,10	A11,12
\mathcal{N}_0	97.5%	90.3%	87.5%	97.5%	86.5%	87.5%
\mathcal{N}_1	97.5%	89.1%	88.3%	97.5%	90.0%	90.0%
\mathcal{N}_2 (MRPN)	97.5%	92.1%	90.8%	97.5%	91.4%	90.0%
RAVDESS	A13,14	A15,16	A17,18	A19,20	A21,22	A23,24
\mathcal{N}_0	82.4%	79.6%	83.2%	89.0%	85.5%	84.2%
\mathcal{N}_1	77.5%	89.1%	86.6%	92.8%	89.1%	90.6%
\mathcal{N}_2 (MRPN)	84.3%	89.7%	89.8%	92.5%	90.6%	90.6%

Our MRPN shows the same or improved recognition performance compared to the \mathcal{N}_0 model as Table 2 and Table 3 illustrate for the sub-datasets. For some subsets, the improvements are not noticeable because the functionality we introduced to the system is only a better correlation function. Thus if the subsets are crystal or fuzzy in both modalities, there can't be improvements only from better correlation functions. Yet still, we can see overall improvements.

Table 3. Comparison for Crema-d of MRPN approach (network \mathcal{N}_2) with simple fusion strategy (\mathcal{N}_0), and advanced fusion strategy (\mathcal{N}_1).

Crema-d	S1	S2	S3	S4	S5
\mathcal{N}_0	77.3%	81.3%	79.2%	74.8%	78.6%
\mathcal{N}_1	72.6%	82.3%	77.3%	74.8%	74.2%
\mathcal{N}_2 (MRPN)	79.5%	83.0%	83.0%	76.8%	81.9%
Crema-d	S6	S7	S8	S9	
\mathcal{N}_0	82.0%	75.1%	79.5%	77.5%	
\mathcal{N}_1	82.0%	74.8%	79.3%	75.8%	
\mathcal{N}_2 (MRPN)	82.0%	80.0%	80.5%	78.6%	

To exhibit the importance of the RP component before our feature fusion layer, we also show the third experimental setting without learnable parameters of RP, noted by \mathcal{N}_1 . The details are in the middle of Figure 7. Such a setting doesn't provide learnable weights for the correlator but forcing the deep features to be multitasking in both single and multi-modal solutions. There are still chances to this purpose yet not stable. The constraints from the multi-branches backpropagation make the system hard to be optimized and can even result in worse performance shown in the Tables.

4.6. Comparing baseline with SOTA

Our proposed MRPN shows state-of-the-art results on both datasets. Though the average improvement of MRPN for both datasets is all around 2% comparing to the common simple fusion of features, it is driven only by eliminating the cross-modal information interference in each modality as Table 2 and Table 3 illustrate. Experiments regarding the pretraining of the CNN extractors and the time augmentation have made the network robust to overcome the overfitting issues regarding the small amount of the training and testing data.

The baseline improvement comparing with others came from good initialization of the CNN extractor components, and the overlapped spectrogram segments as the audio inputs. A similar assumption is drawn by E. Ghaleb [30] where they also applied overlapping in spectrogram segments, but we think the advantage is visible from a better-generalized sequence aggregator when taking this strategy.

Additionally, replacement of LSTM of Bidirectional LSTM and Transformer as aggregator has been conducted but no noticeable differences of them as sequence aggregators can be seen. As for Transformer, the average feature is taken from the decoded outputs, the concept follows from Vision Transformer(ViT)[32].

5. Conclusions

This paper focuses on explaining the cross-modal information interference for the training and testing data in multimodal solutions of the AVER problems.

The reported by other authors (B. Recht [36]) failure of model generalization for *harder cases* of AV data is solved by our MRPN neural network component.

Table 4. Comparison of our fusion models with others recent solutions. Options used: IA – image augmentation, WO – without audio overlapping, VA – video frames augmentation, and AO – audio overlapping. X symbol – there is no report from authors for the given dataset.

Model (our)	RAVDESS	Crema-d
\mathcal{N}_0 (Resnet18+LSTM), IA	83.20%	77.25%
\mathcal{N}_0 (Resnet18+LSTM), WO	85.20%	79.25%
\mathcal{N}_0 (Resnet18+LSTM), VA+AO	87.55%	81.30%
\mathcal{N}_2 (MRPN)(Resnet18+LSTM), VA+AO	90.8%	83.00%
\mathcal{N}_2 (MRPN)(Resnet18+Transformer(avg)), VA+AO	91.4%	83.15%
Model (baseline)	RAVDESS	Crema-d
(OpenFace/COVAREP features + LSTM) + Attention [7]	58.33%	65.00%
Dual Attention + LSTM [30]	67.7%	74.00%
Resnet101 + BiLSTM [33]	77.02%	X
custom CNN [34]	X	69.42%
Early Cross-modal + MFCC + MEL spectrogram [29]	83.6%	X
CNN + Fisher vector + Metric learning [35]	X	66.5%
custom CNN+Spectrogram [21]	79.5%(Audio)	X

The proposed architecture along with the multiple branches loss functions make superior fused features from multi-modal sources. We observe the elimination of inferior cases of multimodal solutions with respect to single modal solutions.

Our results achieve an average accuracy of 91.4% on the RAVDESS dataset and 83.15% on the Crema-d dataset. MRPN solution contributes to a better average recognition rate of approximately 2%. We have observed the maximum improvement for a subset to be around 90% from nearly 80%, while for *easy cases* the recognition rate is already about 97.5%.

The proposed data pre-processing by time augmentation makes general overall rate improvements for both, the single and multi-modal data.

Moreover, the MRPN concept shows its potential for multi-modal classifiers dealing with signal sources not only of optical and acoustical type.

Author Contributions: Conceptualization, X.C. and W.S.; Data curation, X.C.; Formal analysis, X.C. and W.S.; Investigation, X.C. and W.S.; Methodology, X.C. and W.S.; Project administration, X.C. and W.S.; Resources, X.C. and W.S.; Software, X.C. and W.S.; Supervision, W.S.; Validation, X.C. and W.S.; Visualization, X.C. and W.S.; Writing – original draft, X.C. and W.S.; Writing – review & editing, X.C. and W.S.

Funding: Beside statutory support of Warsaw University of Technology this research received no external funding.

Institutional Review Board Statement: Not applicable.

Informed Consent Statement: Not applicable.

Data Availability Statement: The initialization of visual CNN extractor were sampled from the FER-2013 challenge[16]. This data was made available under the Open Database License and can be found at <https://www.kaggle.com/msambare/fer2013>. (accessed on 7 July 2021). The initialization of vocal CNN extractor were sampled from VoxCeleb dataset[28]. This data was made available under the Open Database License and can be found at <https://www.robots.ox.ac.uk/~vgg/data/voxceleb/vox1.html>. (accessed on 7 July 2021). The evaluation of the MRPN and time augmentation is based on RAVDESS dataset[24] and Crema-d[23] under the Open Database License and can be found at <https://zenodo.org/record/1188976#.YOOv3Oj7SUK>(accessed on 7 July 2021) and <https://github.com/CheyneyComputerScience/CREMA-D>(accessed on 7 July 2021) respectively.

Conflicts of Interest: The authors declare no conflict of interest.

Abbreviations

AVER	Audio-video emotion recognition
CNN	Convolution Neural Network
Crema-d [23]	Crowd-sourced Emotional multi-modal Actors Dataset
DNN	Deep Neural Network
HCI	Human-Computer Interaction
FC	FC Fully connected layers
IEMOCAP [20]	Interactive emotional dyadic motion capture dataset
LSTM	Long Short Term Memory
MRPN	multi-modal Residual Perceptron Network
RAVDESS [24]	The Ryerson Audio-Visual Database of Emotional Speech and Song
RP	Residual Perceptron
SAC	Sequence Aggregation Component
SOTA	State of the Art Solution
STFT	Short-term Fourier transformation
SVM	Support Vector Machine
VIT [32]	Vision Transformer

References

1. Belhumeur, P.N.; Hespanha, J.a.P.; Kriegman, D.J. Eigenfaces vs. Fisherfaces: Recognition Using Class Specific Linear Projection. *IEEE Trans. Pattern Anal. Mach. Intell.* **1997**, *19*, 711–720. doi:10.1109/34.598228.
2. Lecun, Y.; Bottou, L.; Bengio, Y.; Haffner, P. Gradient-Based Learning Applied to Document Recognition. *Proceedings of the IEEE*, 1998, pp. 2278–2324.
3. Hochreiter, S.; Schmidhuber, J. Long Short-Term Memory. *Neural Computation* **1997**, *9*, 1735–1780.
4. Vaswani, A.; Shazeer, N.; Parmar, N.; Uszkoreit, J.; Jones, L.; Gomez, A.N.; Kaiser, L.; Polosukhin, I. Attention Is All You Need, 2017, [arXiv:cs.CL/1706.03762].
5. Neverova, N.; Wolf, C.; Taylor, G.W.; Nebout, F. ModDrop: adaptive multi-modal gesture recognition, 2015, [arXiv:cs.CV/1501.00102].
6. Vielzeuf, V.; Pateux, S.; Jurie, F. Temporal Multimodal Fusion for Video Emotion Classification in the Wild, 2017, [arXiv:cs.CV/1709.07200].
7. Beard, R.; Das, R.; Ng, R.W.M.; Gopalakrishnan, P.G.K.; Eerens, L.; Swietojanski, P.; Miksik, O. Multi-Modal Sequence Fusion via Recursive Attention for Emotion Recognition. *Proceedings of the 22nd Conference on Computational Natural Language Learning; Association for Computational Linguistics: Brussels, Belgium*, 2018; pp. 251–259. doi:10.18653/v1/K18-1025.
8. Zadeh, A.; Liang, P.P.; Mazumder, N.; Poria, S.; Cambria, E.; Morency, L.P. Memory Fusion Network for Multi-view Sequential Learning, 2018, [arXiv:cs.LG/1802.00927].
9. Zhang, S.; Zhang, S.; Huang, T.; Gao, W.; Tian, Q. Learning Affective Features With a Hybrid Deep Model for Audio-Visual Emotion Recognition. *IEEE Trans. Cir. and Sys. for Video Technol.* **2018**, *28*, 3030–3043. doi:10.1109/TCSVT.2017.2719043.
10. Tzinis, E.; Wisdom, S.; Remez, T.; Hershey, J.R. Improving On-Screen Sound Separation for Open Domain Videos with Audio-Visual Self-attention, 2021, [arXiv:cs.SD/2106.09669].
11. Wu, Y.; Zhu, L.; Yan, Y.; Yang, Y. Dual Attention Matching for Audio-Visual Event Localization. *Proceedings of the IEEE/CVF International Conference on Computer Vision (ICCV)*, 2019.
12. Noroozi, F.; Marjanovic, M.; Njegus, A.; Escalera, S.; Anbarjafari, G. Audio-Visual Emotion Recognition in Video Clips. *IEEE Transactions on Affective Computing* **2019**, *10*, 60–75. doi:10.1109/TAFFC.2017.2713783.
13. Hossain, M.S.; Muhammad, G. Emotion recognition using deep learning approach from audio-visual emotional big data. *Information Fusion* **2019**, *49*, 69–78. doi:https://doi.org/10.1016/j.inffus.2018.09.008.
14. Ma, F.; Zhang, W.; Li, Y.; Huang, S.L.; Zhang, L. Learning Better Representations for Audio-Visual Emotion Recognition with Common Information. *Applied Sciences* **2020**, *10*, 7239. doi:10.3390/app10207239.
15. Ma, F.; Huang, S.L.; Zhang, L. An Efficient Approach for Audio-Visual Emotion Recognition With Missing Labels And Missing Modalities. *2021 IEEE International Conference on Multimedia and Expo (ICME)*, 2021, pp. 1–6. doi:10.1109/ICME51207.2021.9428219.
16. Goodfellow, I.J.; Erhan, D.; Carrier, P.L.; Courville, A.; Mirza, M.; Hamner, B.; Cukierski, W.; Tang, Y.; Thaler, D.; Lee, D.H.; Zhou, Y.; Ramaiah, C.; Feng, F.; Li, R.; Wang, X.; Athanasakis, D.; Shave-Taylor, J.; Milakov, M.; Park, J.; Ionescu, R.; Popescu, M.; Grozea, C.; Bergstra, J.; Xie, J.; Romaszko, L.; Xu, B.; Chuang, Z.; Bengio, Y. Challenges in representation learning: A report on three machine learning contests. *Neural Networks* **2015**, *64*, 59 – 63. Special Issue on “Deep Learning of Representations”, doi:https://doi.org/10.1016/j.neunet.2014.09.005.

17. Wang, W.; Fu, Y.; Sun, Q.; Chen, T.; Cao, C.; Zheng, Z.; Xu, G.; Qiu, H.; Jiang, Y.G.; Xue, X. Learning to Augment Expressions for Few-shot Fine-grained Facial Expression Recognition, 2020, [[arXiv:cs.CV/2001.06144](https://arxiv.org/abs/2001.06144)].
18. Ng, H.W.; Nguyen, V.D.; Vonikakis, V.; Winkler, S. Deep Learning for Emotion Recognition on Small Datasets Using Transfer Learning. Proceedings of the 2015 ACM on International Conference on Multimodal Interaction; Association for Computing Machinery: New York, NY, USA, 2015; ICMI '15, p. 443–449. doi:10.1145/2818346.2830593.
19. Dhall, A.; Kaur, A.; Goecke, R.; Gedeon, T. EmotiW 2018: Audio-Video, Student Engagement and Group-Level Affect Prediction, 2018, [[arXiv:cs.CV/1808.07773](https://arxiv.org/abs/1808.07773)].
20. Busso, C.; Bulut, M.; Lee, C.C.; Kazemzadeh, A.; Mower Provost, E.; Kim, S.; Chang, J.; Lee, S.; Narayanan, S. IEMOCAP: Interactive emotional dyadic motion capture database. *Language Resources and Evaluation* **2008**, *42*, 335–359. doi:10.1007/s10579-008-9076-6.
21. Mustaqeem.; Kwon, S. A CNN-Assisted Enhanced Audio Signal Processing for Speech Emotion Recognition. *Sensors* **2020**, *20*. doi:10.3390/s20010183.
22. Latif, S.; Rana, R.; Qadir, J.; Epps, J. Variational Autoencoders for Learning Latent Representations of Speech Emotion. *CoRR* **2017**, *abs/1712.08708*, [[1712.08708](https://arxiv.org/abs/1712.08708)].
23. Cao, H.; Cooper, D.G.; Keutmann, M.K.; Gur, R.C.; Nenkova, A.; Verma, R. CREMA-D: Crowd-Sourced Emotional Multimodal Actors Dataset. *IEEE Transactions on Affective Computing* **2014**, *5*, 377–390.
24. Livingstone, S.R.; Russo, F.A. The Ryerson Audio-Visual Database of Emotional Speech and Song (RAVDESS): A dynamic, multimodal set of facial and vocal expressions in North American English. *PLOS ONE* **2018**, *13*, 1–35. doi:10.1371/journal.pone.0196391.
25. Koch, G.; Zemel, R.; Salakhutdinov, R. Siamese Neural Networks for One-shot Image Recognition. 2015.
26. King, D.E. Dlib-Ml: A Machine Learning Toolkit. *J. Mach. Learn. Res.* **2009**, *10*, 1755–1758.
27. He, K.; Zhang, X.; Ren, S.; Sun, J. Deep Residual Learning for Image Recognition. *CoRR* **2015**, *abs/1512.03385*, [[1512.03385](https://arxiv.org/abs/1512.03385)].
28. Nagrani, A.; Chung, J.S.; Zisserman, A. VoxCeleb: A Large-Scale Speaker Identification Dataset. *Interspeech 2017* **2017**. doi:10.21437/interspeech.2017-950.
29. Mansouri-Benssassi, E.; Ye, J. Speech Emotion Recognition With Early Visual Cross-modal Enhancement Using Spiking Neural Networks. 2019 International Joint Conference on Neural Networks (IJCNN), 2019, pp. 1–8. doi:10.1109/IJCNN.2019.8852473.
30. Ghaleb, E.; Popa, M.; Asteriadis, S. Multimodal and Temporal Perception of Audio-visual Cues for Emotion Recognition. 2019 8th International Conference on Affective Computing and Intelligent Interaction (ACII), 2019, pp. 552–558.
31. Tang, R.; Du, M.; Liu, N.; Yang, F.; Hu, X. An Embarrassingly Simple Approach for Trojan Attack in Deep Neural Networks, 2020, [[arXiv:cs.CR/2006.08131](https://arxiv.org/abs/2006.08131)].
32. Dosovitskiy, A.; Beyer, L.; Kolesnikov, A.; Weissenborn, D.; Zhai, X.; Unterthiner, T.; Dehghani, M.; Minderer, M.; Heigold, G.; Gelly, S.; Uszkoreit, J.; Houlsby, N. An Image is Worth 16x16 Words: Transformers for Image Recognition at Scale, 2020, [[arXiv:cs.CV/2010.11929](https://arxiv.org/abs/2010.11929)].
33. Mustaqeem.; Sajjad, M.; Kwon, S. Clustering-Based Speech Emotion Recognition by Incorporating Learned Features and Deep BiLSTM. *IEEE Access* **2020**, *8*, 79861–79875. doi:10.1109/ACCESS.2020.2990405.
34. Ristea, N.; Duțu, L.C.; Radoi, A. Emotion Recognition System from Speech and Visual Information based on Convolutional Neural Networks. 2019 International Conference on Speech Technology and Human-Computer Dialogue (SpeD), 2019, pp. 1–6.
35. Ghaleb, E.; Popa, M.; Asteriadis, S. Metric Learning-Based Multimodal Audio-Visual Emotion Recognition. *IEEE MultiMedia* **2020**, *27*, 37–48. doi:10.1109/MMUL.2019.2960219.
36. Recht, B.; Roelofs, R.; Schmidt, L.; Shankar, V. Do ImageNet Classifiers Generalize to ImageNet?, 2019, [[arXiv:cs.CV/1902.10811](https://arxiv.org/abs/1902.10811)].